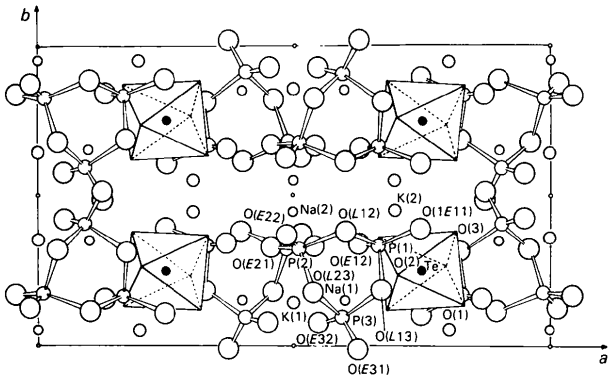

Fig. 1. Projection along the *c* axis of the atomic arrangement of $Te(OH)_6.Na_3P_3O_9.K_3P_3O_9$.

P_3O_9) and $Te(OH)_6$ groups, linked only by hydrogen bonds.

Fig. 1 is a projection of the atomic arrangement on the *ab* plane. H atoms of the $Te(OH)_6$ groups are not represented.

The P_3O_9 *ring anion*

The P_3O_9 ring anions have no internal symmetry. The three P atoms and the bonding O atom (O*L*) are almost coplanar in a plane perpendicular to the *c* axis. These ring planes are distributed in $z \simeq 0{\cdot}0$ and $0{\cdot}5$. All geometrical features of the P_3O_9 group are reported in Table 2 and do not depart significantly from previous observations of other *cyclo*-triphosphates.

The $Te(OH)_6$ *octahedron*

The $Te(OH)_6$ group is centrosymmetric and located around the ($\frac{1}{4}\frac{1}{4}0$, $\frac{1}{4}\frac{3}{4}0$; $\frac{1}{4}\frac{1}{4}\frac{1}{2}$, $\frac{1}{4}\frac{3}{4}\frac{1}{2}$) inversion centres. This group is quite regular, Te—O distances ranging from 1·909 to 1·911 Å.

Associated cation polyhedra

Within a range of 3 Å, the two K atoms are coordinated to eight O atoms. The $K(1)O_8$ polyhedron has a binary symmetry. The two Na atoms have an octahedral oxygen coordination; one of the NaO_6 polyhedra [$Na(2)O_6$] has twofold symmetry.

Geometrical details for the $Te(OH)_6$ group and the associated cation polyhedra are given in Table 2.

The general arrangement of this atomic framework can be simply described by considering the respective locations of $Te(OH)_6$ groups and P_3O_9 rings in planes $z \simeq 0{\cdot}0$ and $0{\cdot}5$. In such planes P_3O_9 anions form an almost regular hexagonal network, each $(P_3O_9)_6$ hexagon being centred by a $Te(OH)_6$ group. The six O atoms of the central $Te(OH)_6$ group are connected by hydrogen bonds to external O atoms of the six different P_3O_9 rings building the surrounding hexagon. Numerical details of the hydrogen-bond scheme are reported in Table 2.

Associated cations are all situated in the intermediate planes ($z \simeq 0{\cdot}25$ and $0{\cdot}75$).

References

BOUDJADA, N. (1981). *Z. Anorg. Allg. Chem.* **477**, 225–228.

BOUDJADA, N. (1985). Thèse d'Etat, Univ. of Grenoble, France.

BOUDJADA, N., AVERBUCH-POUCHOT, M. T. & DURIF, A. (1981*a*). *Acta Cryst.* B**37**, 645–647.

BOUDJADA, N., AVERBUCH-POUCHOT, M. T. & DURIF, A. (1981*b*). *Acta Cryst.* B**37**, 647–649.

BOUDJADA, N., BOUJADA, A. & GUITEL, J. C. (1983). *Acta Cryst.* C**39**, 656–658.

BOUDJADA, N. & DURIF, A. (1982). *Acta Cryst.* B**38**, 595–597.

BOUDJADA, N., LAMBERT-ANDRON, B. & BOUCHERLE, J. X. (1985). *Z. Kristallogr.* **172**, 45–53.

Enraf–Nonius (1977). *Structure Determination Package.* Enraf–Nonius, Delft, The Netherlands.

International Tables for X-ray Crystallography (1974). Vol. IV. Birmingham: Kynoch Press. (Present distributor D. Reidel, Dordrecht.)

Acta Cryst. (1987). C**43**, 1655–1659

Structural Phase Transitions in Chevrel Phases Containing Divalent Metal Cations. I. Structure Refinement of Rhombohedral $M Mo_6S_8$ (M = Eu, Sr, Ba) at Room Temperature

BY F. KUBEL AND K. YVON

Laboratoire de Cristallographie aux Rayons X, Université de Genève, 24 quai Ernest-Ansermet, CH-1211 Genève 4, Switzerland

(*Received* 19 *March* 1986; *accepted* 29 *September* 1986)

Abstract. Single-crystal X-ray diffraction data on $M Mo_6S_8$ (M = Eu, Sr, Ba) at $T = 294$ K and ambient pressure are reported: $M_r = 984{\cdot}1$, 919·8, 969·5, space group $R\bar{3}$, Mo $K\alpha$ radiation ($\lambda = 0{\cdot}71069$ Å), $a_{rh} =$ 6·5535 (2), 6·5702 (3), 6·6507 (3) Å, $\alpha = 88{\cdot}918$ (3), 89·003 (5), 88·584 (6)°, $V = 281{\cdot}32$ (2), 283·50 (3), 293·90 (4) Å^3, $Z = 1$, $D_x = 5{\cdot}809$, 5·387, 5·477 Mg m^{-3}, $\mu = 13{\cdot}21$, 12·18, 10·68 mm^{-1}, $F(000)$

0108-2701/87/091655-05$01.50

= 443, 418, 436, R = 0·021, 0·035, 0·019, wR = 0·024, 0·040, 0·030, for 2550 (Eu), 1836 (Sr), 1677 (Ba) independent reflections. The structures MMo$_6$S$_8$ (M = Eu, Sr, Ba) differ mainly with respect to the bond distances and bond angles between the [Mo$_6$S$_8$] units: d(Mo–Mo)$_{inter}$ = 3·28, 3·30, 3·41 Å and d(Mo–S)$_{inter}$ = 2·58, 2·59, 2·62 Å, S–Mo–S = 99·9, 99·3, 96·5°; the metal–sulfur bond distances: d(M–S) = 2·83, 2·84, 2·97 Å; and the anisotropy of the thermal vibrations of the M atoms: $U_\perp/U_{||}$ = 3·4, 2·4, 2·4. By contrast the bond distances within the [Mo$_6$S$_8$] units, and in particular those within the Mo$_6$ clusters are practically identical: d(Mo–Mo)$_{intra}$ (Å) = 2·666, 2·717 (Eu); 2·666, 2·712 (Sr); 2·667, 2·703 (Ba).

Introduction. Chevrel-phase sulfides MMo$_6$S$_8$ (M = metal) containing divalent metal cations such as Pb^{2+} and Sn^{2+} show high superconductive transition temperatures (for a review see Fischer, 1978). The absence of superconductivity in compounds containing other divalent metal cations such as Eu^{2+} and the alkaline earths Ca^{2+}, Sr^{2+} and Ba^{2+} remained a puzzle until low-temperature X-ray diffraction, electrical resistivity and specific heat measurements revealed the occurrence of structural phase transitions (Baillif, Dunand, Muller & Yvon, 1981; Baillif, Junod, Lachal, Muller & Yvon, 1981; Lachal, Baillif, Junod & Muller, 1983). The compounds of this series are also of interest from a crystal chemistry point of view because they yield insight into the interplay between electronic and geometric factors which are important for the metal–metal bonding (Corbett, 1981).

In this series of articles we report on the structural characterization of these compounds at various temperatures. In the first part we present single-crystal X-ray diffraction data at room temperature on the rhombohedral high-temperature phase of the sulfides MMo$_6$S$_8$ based on M = Eu, Sr and Ba. These compounds are particularly favourable for a study of geometric factors because of their similar electronic configurations. For example they allow the study of the structural response of the Mo$_6$ clusters to changes in the nonmetal matrix induced by substitution of M atoms of different size and equal valency.

Experimental. Well characterized samples of nominal composition MMo$_6$S$_8$ (M = Eu, Sr, Ba) were supplied by R. Baillif. They were synthesized by a preliminary reaction of the elements in a quartz tube at 1300 K and subsequent melting in a high-pressure furnace at 0·2 GPa Ar pressure (Baillif, Junod, Lachal, Muller & Yvon, 1981). X-ray Guinier photographs and metallographic examination confirmed that the samples were well crystallized and contained no significant concentrations of impurity phases. SrMo$_6$S$_8$ and BaMo$_6$S$_8$ single crystals of approximately cubic shape were isolated from crushed samples, whereas EuMo$_6$S$_8$ crystals of approximately spherical shape were prepared by grinding crystal fragments in a diamond-coated compressed-air mill. All crystals were examined on automated four-circle X-ray diffractometers. Cell parameters were determined by least-squares refinement of 25 (Eu, Ba) and 20 (Sr) measured Bragg angles in the region $45 \le \theta \le 58°$ (Eu), $27 \le \theta \le 29°$ (Sr) and $30 \le \theta \le 38°$ (Ba). Absorption effects were corrected empirically from azimuthal scans of nine reflections. The structures were refined by the *XRAY* program system (Stewart, Machin, Dickinson, Ammon, Heck & Flack, 1976) and the *SDP* program system (Frenz, 1983), by minimizing the function $\sum w_i(|F_r|_i - |F_c|_i/k_i)^2$ with $w_i = 1/\sigma^2(F_r)_i$. The starting values for the atomic coordinates were those reported for PbMo$_6$S$_8$ (Marezio, Dernier, Remeika, Corenzwit & Matthias, 1973). In order to allow comparison with the coordinates of the triclinic low-temperature modifications they were transformed to those corresponding to a rhombohedral description of the structure (space group $R\bar{3}$; *International Tables for Crystallography,* 1983). Convergence was considered complete when the refined parameters did not vary by more than 10^{-5}. Atomic scattering factors and anomalous-dispersion factors were taken from *International Tables for X-ray Crystallography* (1974). The cell parameters, measurement conditions, weights, absorption and extinction coefficients, the number of parameters refined, and the agreement indices at convergence are summarized in Table 1. The results of the refinements* are summarized in Table 2, and structural drawings are given in Figs. 1 and 2. Interatomic distances and angles are summarized in Table 3. For EuMo$_6$S$_8$ and BaMo$_6$S$_8$ the precision of the atomic coordinates is the highest reported so far for Chevrel-phase structures. Final electron density difference maps showed features which did not exceed 3·8 (Eu), 4·3 (Sr), 4·2 e Å^{-3} (Ba). Refinements based on variable site-occupancy factors gave no indication of the possible occurrence of defects in any of the crystals.

Discussion. The structural features of Chevrel phases have been abundantly discussed in the literature (for reviews see Yvon, 1978, 1982; Corbett, 1981; Chevrel & Sergent, 1982). Their basic structural units are cube-shaped [Mo$_6$S$_8$] units which contain octahedral Mo$_6$ clusters (point-group symmetry $\bar{3}$) and are linked *via* short Mo–S intercluster bonds to a three-dimensional rhombohedral network (Fig. 1). Large metal atoms M such as those considered in this work (M = Eu, Sr, Ba) occupy interstices in the chalcogen-atom network which are formed by six 'peripheral'

* Lists of structure factors have been deposited with the British Library Document Supply Centre as Supplementary Publication No. SUP 43358 (84 pp.). Copies may be obtained through The Executive Secretary, International Union of Crystallography, 5 Abbey Square, Chester CH1 2HU, England.

[S(1)] and two 'axial' [S(2)] atoms and have the shape of a more-or-less compressed cube (point-group symmetry $\bar{3}$). A structural detail of particular interest is the Mo_6 cluster which is believed to be important for superconductivity (Fischer, 1978; Andersen, Klose & Nohl, 1978). As shown in previous work (Yvon, 1978), its size and elongation (along $\bar{3}$) varies in a characteristic manner as a function of metal-atom (M) insertion or substitution, *i.e.* the cluster contracts and becomes more regular as the valency and concentration of M is increased. This behaviour was interpreted in terms of two effects, of which one is essentially of electronic and the other of geometric origin. The former invokes charge transfer from the metal to the nonmetal atoms which determines the valence-electron concentration on the Mo_6 cluster (cluster-VEC) and thus the number of electrons available for metal–metal bonding (Yvon, 1978). The latter effect invokes repulsive interactions between the chalcogen atoms (matrix effect) which influence the metal–metal bonding *via* the network of metal–nonmetal bonds (Corbett, 1981). The relative importance of these two effects has so far not been established, partly because of correlations which exist between the size and the valency of the inserted metal cations M, the possibly different electronic behaviour of sulfur-, selenium- and tellurium-based congeners (Nohl, Klose & Andersen, 1982), and the lack of structural data for compounds having either equal nonmetal matrix or equal cluster-VEC.

The compounds belonging to the series $M\mathrm{Mo_6S_8}$ (M = Eu, Sr, Ba) afford a favourable ground for study of the matrix effect because their cluster-VEC's are equal (22e/Mo_6). In particular they allow the study of the structural response of the chalcogen-atom network and the Mo_6 clusters to substitution of metal (M) cations of different size [$r_{M^{2+}}$ (Å) = 1·17 (Eu), 1·18 (Sr), 1·35 (Ba); Shannon, 1976]. As shown in Fig. 2 the most important structural response occurs in the immediate vicinity of the M atoms. Substitution of Eu^{2+} by Sr^{2+} and Ba^{2+} leads to an anisotropic expansion (mainly along $\bar{3}$) of the local sulfur-atom environment, *i.e.* the axial M–S(2) bonds (bond label *i* in Fig. 2*a*) are stretched by 0·14 Å whereas the peripheral M–S(1) bonds (bond label *j*) are stretched by 0·10 Å. This anisotropic expansion is partly compensated by structural changes in the regions *between* (Fig. 2*b*) and *within* (Fig. 2*c*) the [Mo_6S_8] units. As shown in Fig. 2(*b*), the rhomboid generated by Mo–S(1) intracluster bonds (label *d*) and Mo–S(1) intercluster bonds (label *h*), *i.e.* that bisected by the Mo–Mo intercluster bond

Table 1. *Experimental conditions and agreement factors for* $M\mathrm{Mo_6S_8}$ (M = Eu, Sr, Ba) *with e.s.d.'s in parentheses*

	$EuMo_3S_8$	$SrMo_6S_8$	$BaMo_6S_8$
Lattice parameters			
a_{rh} (Å)	6·5535 (2)	6·5702 (3)	6·6507 (3)
α (°)	88·918 (3)	89·003 (5)	88·584 (6)
V_{th} (Å^3)	281·32 (2)	283·50 (3)	293·90 (4)
a_{hex} (Å)	9·1801 (3)	9·2105 (6)	9·2881 (7)
c_{hex} (Å)	11·5635 (6)	11·5763 (10)	11·8004 (10)
V_{hex} (Å^3)	843·96 (6)	850·50 (10)	881·70 (11)
Crystal radius (mm)	0·10	0·09	0·09
μ (mm^{-1})	13·21	12·18	10·68
Wavelength (Å)	0·71069	0·71069	0·71069
$(\sin\theta/\lambda)_{max}$ (Å^{-1})	1·28	1·08	1·08
Range of *hkl*			
h	−11→11	−11→10	−9→10
k	−14→6	−10→11	−14→7
l	−8→16	−5→14	−7→14
Standard reflections	$\bar{3}\bar{3}0$	$\bar{3}\bar{3}6$	444
	$4\bar{2}4$	$4\bar{2}4$	215
	$4\bar{6}\bar{4}$	060	
Max. intensity variation of standard reflections	1·5%	1·3%	2·6%
R_{int}	2·0%	0·5%	1·9%
wR_{int}	2·5%	1·0%	2·1%
Max. shift/e.s.d.	<10^{-2}	<10^{-2}	<10^{-2}
Scan type	ω–2θ	ω–2θ	ω–2θ
Scan speed (° min^{-1})	3·5–5·5*	1·2	3·5–5·5*
Number of reflections measured	7284	2371	5968
Number of independent reflections	2550	1839	1677
R	2·1%	3·5%	1·9%
wR	2·4%	4·0%	3·0%
Goodness-of-fit	6·18	7·51	1·03
Diffractometer	CAD-4	Philips	CAD-4
Extinction coefficient (° ×10^{-6})	3·31 (7)	10·7 (2)	1·41 (4)

* Depending on prescan intensity, $I_{final} > 33\sigma_{I\,prescan}$ and $T < 60$ s.

Table 2. *Atomic coordinates and anisotropic thermal parameters* U_{ij} (Å^2 ×10^2) *of* $M\mathrm{Mo_6S_8}$ (M = Eu, Sr, Ba) *with e.s.d.'s in parentheses*

Space group $R\bar{3}$, rhombohedral setting. The expression of temperature factors is: $\exp[-2\pi^2(h^2a^{*2}U_{11} + k^2b^{*2}U_{22} + l^2c^{*2}U_{33} + 2hka^*b^*U_{12} + 2hla^*c^*U_{13} + 2klb^*c^*U_{23})]$, where a^*, b^*, c^* are reciprocal lattice constants.

	$EuMo_6S_8$	$SrMo_6S_8$	$BaMo_6S_8$
M in 1*a* [0,0,0]			
U_{11}	1·351 (3)	1·35 (2)	1·153 (3)
U_{12}	−0·427 (2)	−0·34 (1)	−0·298 (3)
$U_{\perp}$†	1·744 (4)	1·66 (2)	1·401 (5)
$U_{\parallel}$†	0·514 (5)	0·70 (3)	0·583 (5)
Mo in 6*f* [*x*,*y*,*z*]			
x	0·22851 (2)	0·22964 (4)	0·23459 (2)
y	0·41817 (2)	0·41819 (3)	0·41754 (2)
z	0·56283 (2)	0·56293 (4)	0·56556 (2)
U_{11}	0·533 (2)	0·60 (1)	0·645 (4)
U_{22}	0·493 (2)	0·55 (1)	0·570 (4)
U_{33}	0·506 (2)	0·56 (1)	0·603 (4)
U_{12}	−0·017 (2)	0·012 (8)	−0·031 (3)
U_{13}	−0·048 (2)	−0·015 (8)	−0·065 (3)
U_{23}	−0·044 (2)	−0·001 (8)	−0·039 (3)
S(1) in 6*f* [*x*,*y*,*z*]			
x	0·38217 (6)	0·3829 (1)	0·39031 (7)
y	0·12491 (5)	0·1251 (1)	0·12297 (7)
z	0·74359 (6)	0·7416 (1)	0·73598 (7)
U_{11}	0·846 (9)	0·96 (3)	1·02 (1)
U_{22}	0·550 (8)	0·66 (3)	0·65 (1)
U_{33}	0·828 (9)	0·92 (3)	0·95 (1)
U_{12}	−0·093 (7)	−0·08 (3)	−0·14 (1)
U_{13}	0·039 (8)	0·09 (3)	0·05 (1)
U_{23}	0·053 (7)	0·10 (2)	0·09 (1)
S(2) in 2*c* [*x*,*x*,*x*]			
x	0·2448 (2)	0·2454 (1)	0·2515 (2)
U_{11}	0·89 (2)	1·06 (2)	1·13 (3)
U_{12}	−0·25 (2)	−0·26 (2)	−0·35 (3)
$U_{\perp}$†	1·11 (2)	1·29 (4)	1·45 (2)
$U_{\parallel}$†	0·41 (2)	0·57 (5)	0·44 (2)

† Values ⊥ and ∥ to the ternary axis as obtained from a refinement in hexagonal setting.

(label *c*; see also Fig. 2 in the work of Corbett, 1981), is stretched along the Mo–Mo bond axis such that the Mo–Mo intercluster separation increases by 0·14 Å, and the Mo–S(1) intercluster bond distance (bond label *h*) by 0·04 Å, while two of the S–Mo–S bond angles (β and γ) change by up to 3·39°, and one of the nonbonding S(1)–S(1) contact distances (label *k*; marked by a dotted line in Fig. 2*b*) by 0·08 Å.

The changes within the [Mo$_6$S$_8$] units concern mainly the nonbonding S–S contact distances. Those between the axial and peripheral S atoms (bond label *m* in Fig. 2*c*) decrease by 0·024 Å, while those between the peripheral S atoms (bond label *n*) increase by 0·030 Å. In contrast the Mo–S bond distances (*d*, *e*, *f*, *g*) and S–Mo–S bond angles (δ and ε) remain practically unchanged (maximum differences of 0·014 Å and 1·25°, respectively). Furthermore the size and elongation of the Mo$_6$ clusters is nearly unaffected by *M*-atom substitution (bond labels *a* and *b* in Fig. 2*c*). As the lattice expands the clusters show a tendency to contract as expected from both the matrix effect (relief of nonbonding S–S interactions) and the electronic effect (weakening of Mo–Mo intercluster bonds), but the contraction is very small (about 0·01 Å), showing that these clusters respond only marginally to an *average* relief of nonbonding S–S interactions (the average between the S–S contact distances *l* and *k* increases by 0·04 Å across the series). The size and elongation of these clusters are practically identical to those in other 22-electron sulfides such as PbMo$_6$S$_8$ [d(Mo–Mo)$_{intra}$ = 2·73, 2·68 Å] and SnMo$_6$S$_8$ (2·74, 2·68 Å), but smaller than those in 21-electron sulfides such as AgMo$_6$S$_8$ (2·80, 2·71 Å) and larger than those in 24-electron sulfides such as Cu$_{\sim 4}$Mo$_6$S$_8$ (2·71, 2·66 Å) (Yvon, 1978; Chevrel & Sergent, 1982). A similar trend was also observed for Chevrel-phase selenides in which electron-rich metal clusters such as in Mo$_4$Ru$_2$Se$_8$ {24 valence electrons, d[(Mo,Ru)–(Mo,Ru)]$_{intra}$ = 2·71, 2·66 Å} were anomalously small compared to those in electron-poor metal clusters such as in Mo$_6$Se$_8$ [20 valence electrons, d(Mo–Mo)$_{intra}$ = 2·69, 2·84 Å] (Hönle, Flack & Yvon, 1983). These observations are consistent with the role attributed to the electronic (charge-transfer) effect. However, they do not imply that matrix effects do not play a role in the alkaline-earth series. In fact the *shortest* S–S contact distance in their structure (label *l*, indicated by a dotted line in Fig.

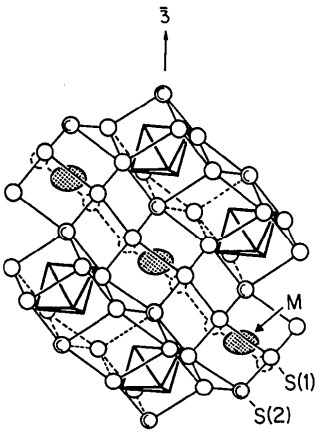

Fig. 1. Projection of MMo$_6$S$_8$ (M = Eu, Sr, Ba) approximately perpendicular to the trigonal axis. Thick lines: Mo$_6$ cluster; thin lines: S–S contacts; open circles: S; shaded circles: M atoms. For structural details, bond lengths and bond angles see Fig. 2 and Table 3.

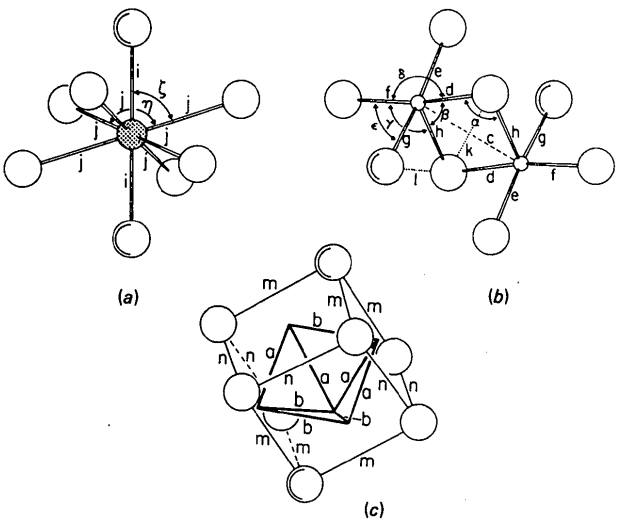

Fig. 2. Sulfur-atom environment around an M atom (*a*), structural region between two [Mo$_6$S$_8$] units (*b*), and [Mo$_6$S$_8$] unit (*c*) in MMo$_6$S$_8$ (M = Eu, Sr, Ba). Open circles: S; shaded circles: M atoms; thick lines Mo$_6$ cluster. For values of interatomic distances and bond angles (marked by arabic and greek letters, respectively) see Table 3.

Table 3. *Interatomic distances and angles in* MMo$_6$S$_8$ (M = Eu, Sr, Ba) *with e.s.d.'s in parentheses*

		EuMo$_6$S$_8$	SrMo$_6$S$_8$	BaMo$_6$S$_8$
Distances* (Å)				
1. Mo–Mo	*a*:	2·7173 (2)	2·7115 (4)	2·7026 (2)
	b:	2·6659 (2)	2·6661 (4)	2·6673 (2)
	c:	3·2768 (2)	3·2997 (4)	3·4086 (3)
2. Mo–S	*d*:	2·5082 (4)	2·5050 (8)	2·4976 (5)
	e:	2·4612 (4)	2·4617 (8)	2·4750 (5)
	f:	2·4489 (4)	2·4485 (8)	2·4583 (5)
	g:	2·3925 (2)	2·3918 (7)	2·3854 (2)
	h:	2·5817 (4)	2·5893 (8)	2·6181 (5)
3. M–S	*i*:	2·8304 (6)	2·8413 (7)	2·9681 (8)
	j:	3·1037 (4)	3·1245 (7)	3·2092 (5)
4. S–S	*k*:	3·8955 (6)	3·882 (1)	3·8166 (7)
	l:	3·4101 (8)	3·4191 (9)	3·405 (1)
	m:	3·4788 (5)	3·4721 (7)	3·4549 (6)
	n:	3·4402 (5)	3·445 (1)	3·4700 (7)
Angles* (°)				
1. Mo–S–Mo	α:	80·14 (1)	80·72 (2)	83·53 (1)
2. S–Mo–S	β:	99·86 (1)	99·28 (2)	96·47 (2)
	γ:	88·97 (1)	89·31 (2)	91·27 (2)
	δ:	171·00 (1)	171·30 (2)	172·25 (2)
	ε:	91·86 (1)	91·66 (2)	90·99 (2)
3. S–M–S	ξ:	71·86 (1)	72·04 (2)	72·21 (1)
	η:	69·23 (1)	69·06 (2)	68·90 (1)

* For symbols see Fig. 2.

2*b*) remains practically unaffected by *M*-atom substitution. Thus this particular matrix element could also be of importance for the Mo_6-cluster geometry.

Further structural features which change significantly upon *M*-atom substitution are the amplitudes of thermal vibrations of the *M* and axial chalcogen [S(2)] atoms. They show strong anisotropy (see $U_\perp$ and $U_{||}$ values in Table 2). The vibrations of the *M* atoms are up to three times larger parallel to than perpendicular to the ternary axis. As expected from the topology of the structure those of the axial S(2) atom ligands follow these vibrations. Those perpendicular to the ternary axis [$U_\perp = 0{\cdot}01744$ (Eu), 0·0166 (Sr), 0·01401 Å^2 (Ba)] correlate with the lattice transformation temperatures, $T_l = 109$ (Eu), 139 (Sr), 171 K (Ba).

Note added in proof: Structure parameters were recently reported for $EuMo_6S_8$ (Peña, Horyn, Geantet, Gougeon, Padiou & Sergent, 1986). They do not differ significantly from those reported above. Their precision is lower by a factor of two, on the average.

We thank Dr R. Baillif for supplying the samples and Dr A. Dunand for preliminary measurements. This work was supported by the Swiss National Science Research Foundation under contract 2615-0.85.

References

ANDERSEN, O. K., KLOSE, W. & NOHL, H. (1978). *Phys. Rev. B*, 17, 1209–1237.

BAILLIF, R., DUNAND, A., MULLER, J. & YVON, K. (1981). *Phys. Rev. Lett.* **47**, 672–675.

BAILLIF, R., JUNOD, A., LACHAL, B., MULLER, J. & YVON, K. (1981). *Solid State Commun.* **40**, 603–606.

CHEVREL, R. & SERGENT, M. (1982). *Superconductivity in Ternary Compounds*, Vol. 1, edited by Ø. FISCHER & M. B. MAPLE, pp. 25–86. Berlin: Springer-Verlag.

CORBETT, J. D. (1981). *J. Solid State Chem.* **39**, 56–74.

FISCHER, Ø. (1978). *Appl. Phys.* **16**, 1–28.

FRENZ, B. A. (1983). *Enraf–Nonius Structure Determination Package*. Enraf–Nonius, Delft.

HÖNLE, W., FLACK, H. D. & YVON, K. (1983). *J. Solid State Chem.* **49**, 157–165.

International Tables for Crystallography (1983). Vol. A. Dordrecht: D. Reidel.

International Tables for X-ray Crystallography (1974). Vol. IV. Birmingham: Kynoch Press. (Present distributor D. Reidel, Dordrecht.)

LACHAL, B., BAILLIF, R., JUNOD, A. & MULLER, J. (1983). *Solid State Commun.* **45**, 849–851.

MAREZIO, M., DERNIER, P. D., REMEIKA, J. P., CORENZWIT, E. & MATTHIAS, B. T. (1973). *Mater. Res. Bull.* **8**, 657–668.

NOHL, H., KLOSE, W. & ANDERSEN, O. K. (1982). *Superconductivity in Ternary Compounds*, Vol. 1, edited by Ø. FISCHER & M. B. MAPLE, pp. 165–221. Berlin: Springer-Verlag.

PEÑA, O., HORYN, R., GEANTET, C., GOUGEON, P., PADIOU, J. & SERGENT, M. (1986). *J. Solid State Chem.* **63**, 62–69.

SHANNON, R. D. (1976). *Acta Cryst.* A**32**, 751–767.

STEWART, J. M., MACHIN, P. A., DICKINSON, C. W., AMMON, H. L., HECK, H. & FLACK, H. (1976). The *XRAY76* system. Tech. Rep. TR-446. Computer Science Center, Univ. of Maryland, College Park, Maryland.

YVON, K. (1978). *Current Topics in Materials Science*, Vol. 3, edited by E. KALDIS, pp. 53–129. Amsterdam: North-Holland.

YVON, K. (1982). *Superconductivity in Ternary Compounds*, Vol. 1, edited by Ø. FISCHER & M. B. MAPLE, pp. 87–111. Berlin: Springer-Verlag.

Acta Cryst. (1987). C**43**, 1659–1661

Structure of an Ammonium Lead Polyphosphate

BY B. M. GATEHOUSE AND L. W. GUDDAT

Chemistry Department, Monash University, Clayton, Victoria 3168, *Australia*

(*Received* 11 *March* 1987; *accepted* 21 *April* 1987)

Abstract. $NH_4Pb(PO_3)_3$, $M_r = 462{\cdot}2$, monoclinic, $P2_1/c$, $a = 7{\cdot}214\,(2)$, $b = 17{\cdot}062\,(3)$, $c = 14{\cdot}157\,(2)$ Å, $\beta = 105{\cdot}30\,(2)°$, $V = 1680{\cdot}8$ Å^3, $Z = 8$, D_m not measured (insufficient material), $D_x = 3{\cdot}65$ Mg m^{-3}, λ(Mo $K\bar{\alpha}$) = 0·7107 Å, $\mu = 207{\cdot}5$ mm^{-1}, $F(000) = 1680$, $T = 293$ K, final $R = 0{\cdot}066$ for 3446 counter-measured reflections. The structure consists of infinite contorted $(PO_3)_n$ chains containing six unique phosphorus–oxygen tetrahedra separated by lead–oxygen polyhedra, one seven and one eight coordinate, and ammonium ions. The mean P—O and Pb—O distances are 1·544 and 2·655 Å respectively.

Introduction. Following from an interest in compounds containing chains or polyanions of the type $E_4O_{13}^{n-}$, the structure of $Ba_3V_4O_{13}$ was recently determined (Gatehouse, Guddat & Roth, 1987). The unit-cell dimensions of this compound and of low- and high-temperature $Ba_3P_4O_{13}$ were reported recently (Millet, Parker & Roth, 1986), as was a method of preparation of $Pb_3P_4O_{13}$ (Averbuch-Pouchot & Durif, 1986). During attempts to prepare single crystals of the latter compound, crystals of another material, that proved to be $NH_4Pb(PO_3)_3$, were obtained. The structure of this compound is reported here.

0108-2701/87/091659-03$01.50